

## Spinodal decomposition in a three-dimensional fluid model

Oriol T. Valls

*School of Physics and Astronomy, University of Minnesota, Minneapolis, Minnesota 55455  
and Minnesota Supercomputer Institute, University of Minnesota, Minneapolis, Minnesota 55455*

James E. Farrell

*School of Physics and Astronomy, University of Minnesota, Minneapolis, Minnesota 55455  
and Department of Chemical Engineering, University of California, Santa Barbara, California 93106*

(Received 12 March 1992)

We study spinodal decomposition after a critical quench to finite temperature for a three-dimensional Langevin fluid model which includes the full couplings between the order parameter and the currents. Our results agree with the expectation based on phenomenological considerations, namely, that the asymptotic growth exponent for this model is  $n=1$ , and, when compared to two-dimensional results for the same model, indicate that the dimensionality may be relevant in this problem.

PACS number(s): 64.60.My, 64.60.Cn, 64.70.Fx

Spinodal decomposition (SD) is the process of phase separation and domain growth which occurs after a system is placed (e.g., by means of a temperature quench) in an unstable region of its phase diagram. It has been experimentally studied both in fluid systems [1] and in binary alloys [2]. Beyond an initial transient when domains first form, their size  $l(t)$  is characterized as a function of time by a function which at long times is typically a power law  $l(t) \sim t^n$ , where  $n$  is called the growth exponent. The determination of  $n$  at "asymptotic" times, and the classification of SD phenomena into "universality classes" possibly depending on dimensionality and on certain relevant system characteristics, have been the object of much study.

One of the relevant factors which influences the growth law is the presence of currents. In simple fluid systems, two time regimes [1] are observed: At relatively early times, a power law with an exponent  $n \approx 0.3 \sim 0.4$  is seen, which changes to  $n \approx 1$  at later times. Only one regime, with small  $n$ , is seen in alloys. The behavior in the fluid case is generally understood in terms of the hydrodynamic phenomenology developed in Ref. [3], where it is shown that an early  $n = \frac{1}{3}$  exponent should change to  $n=1$  because of the formation of cylindrical domain structures.

Extensive numerical work on SD has been done. Here we focus on a three-dimensional Langevin equation model for a fluid, incorporating currents and temperature fluctuations. Within the Langevin-equation context, and for quenches through the critical point (the case studied here) it is well established that for model B (in the usual taxonomy [4]), where the only variable is the order-parameter

density, the exponent  $n$  is  $n \approx 0.3$  in two dimensions ( $d=2$ ) [5]. At  $d=3$  the same result has been established [6], although only for quenches to zero temperature. These results apply to alloys. For fluids, an extensive study [7,8] of SD for a Langevin model including coupling to hydrodynamic currents (an extension of model H [4]) has been performed at  $d=2$ , where it was found that for critical quenches, there are two regimes for  $n$ . One has  $n \approx 0.3$  at earlier times, increasing to a value of  $n \approx 0.69$  at the latest times considered. Since the hydrodynamic arguments of Ref. [3] are specifically tied to  $d=3$  (indeed, hydrodynamic behavior at  $d=2$  is quite another story) it is not well established whether  $d$  is a "relevant parameter" for fluid spinodal decomposition.

In this Rapid Communication, we present results, in three dimensions, for critical quenches to finite temperature for precisely the same model studied in Ref. [7]. These are the first  $d=3$  results obtained for these quenches within a model that explicitly contains a hydrodynamic current, and the appropriate associated convection terms, coupled to the order parameter [9]. Our results can be directly compared to those of model B (in two or three dimensions) and to the two-dimensional results for the same model [7]. We find that they support the phenomenological theory of Ref. [3], in agreement with experiment.

The model equations that we use were derived in Ref. [7] from the appropriate  $\phi$  and  $\mathbf{j}$ -dependent free-energy functional, using standard procedures. Defining appropriate units of length and time, they can be written in dimensionless form as

$$\partial_t \phi(\mathbf{r}, t) = \nabla^2 [\phi^3(\mathbf{r}, t) - \phi(\mathbf{r}, t) - \nabla^2 \phi(\mathbf{r}, t)] - g \nabla \cdot [\phi(\mathbf{r}, t) \mathbf{j}(\mathbf{r}, t)] + \mu(\mathbf{r}, t), \quad (1a)$$

$$\begin{aligned} \partial_t j_i(\mathbf{r}, t) = & \eta \nabla^2 j_i(\mathbf{r}, t) + \sigma \sum_k \nabla_i \nabla_k j_k(\mathbf{r}, t) - g \phi(\mathbf{r}, t) \nabla_i [\phi^3(\mathbf{r}, t) - \phi(\mathbf{r}, t) - \nabla^2 \phi(\mathbf{r}, t)] \\ & - g \sum_k \{ \nabla_k [j_i(\mathbf{r}, t) j_k(\mathbf{r}, t)] + j_k(\mathbf{r}, t) \nabla_i j_k(\mathbf{r}, t) \} + v_i(\mathbf{r}, t). \end{aligned} \quad (1b)$$

All quantities in Eq. (1) are dimensionless.  $\phi$  and  $\mathbf{j}$  are the order-parameter and current fields, respectively,  $\eta$  is the dimensionless shear viscosity and  $\sigma = \frac{1}{3}\eta + \zeta$ , where  $\zeta$  is the dimensionless bulk viscosity. The quantities  $\mu$  and  $\mathbf{v}$  are Gaussian noise fields satisfying

$$\langle \mu(\mathbf{r}, t) \mu(\mathbf{r}', t') \rangle = -2\epsilon \nabla^2 \delta^3(\mathbf{r} - \mathbf{r}') \delta(t - t'), \quad (2a)$$

$$\langle v_i(\mathbf{r}, t) v_k(\mathbf{r}', t') \rangle = -2\epsilon (\eta \nabla^2 \delta_{i,k} + \sigma \nabla_i \nabla_k) \times \delta^3(\mathbf{r} - \mathbf{r}') \delta(t - t'). \quad (2b)$$

In (2)  $\epsilon$  is the noise strength (dimensionless temperature). In (1) the parameter  $g$  is the coupling between order parameter and current. At  $g=0$  one recovers model B. Here, as in Refs. [7,8], we shall set  $g=1$ . This model is an extension of "model H," as discussed in Refs. [7,8]. The first two terms on the right-hand side of (1b) are viscous drag terms from the Navier-Stokes equation. The remaining terms include the convective derivative and additional nonlinear couplings. In general, a full description of a fluid system requires coupling to an additional scalar field representing the pressure fluctuations [10], coupled to  $\phi(\mathbf{r}, t)$  through the longitudinal part of the current. However, it was shown in Ref. [8] that this additional term does not change the two-dimensional results.

The parameters in the problem are (besides  $g$ )  $\eta$ ,  $\sigma$ , and  $\epsilon$ . We have taken  $\eta=1$ ,  $\sigma=2$ , and  $\epsilon=0.1$ . These values are exactly the same as those used in two dimensions in Ref. [7], and allow direct comparison of  $d=2$  and  $d=3$  results. Note that we do not assume that the temperature is irrelevant, as has been done in the three-dimensional work on model B [6]. We know of no arguments that would warrant such an assumption for model H, and the assumption seems to us in any case of relatively little value in simplifying the problem: Several runs are necessary even at  $T$  (or  $\epsilon$ ) = 0 to average over random initial conditions. The computer-time savings associated with not having to generate noise fields are partly negated by the fact that domain growth is more rapid in the presence of temperature fluctuations. Further, given the very highly nonlinear nature of our equations, the danger of reaching special solutions when solving (at  $T=0$ ) a set of deterministic equations is hard to contend with.

We have utilized here precisely the same numerical procedures developed in Refs. [7,8] (and references therein) and will not discuss them again in this work. We use a cubic lattice of size  $N^3$ . We have found, by experimenting with relatively small system sizes, that finite-size effects set in when the domain size (as specified below) is about  $\sim 0.2N$  where  $N$  is the lattice size. We have performed 50 runs at  $N=50$ , which allows us to study the intermediate-time behavior up to  $t \approx 120$ . These results will be reported elsewhere [11]. Here we will focus on results for six runs at  $N=81$ , which allows  $t=300$  to be reached before finite-size effects are encountered. This size compares favorably with  $N=66$  used in three-dimensional model B work [6]. The time step needed is  $\delta t = 0.01$ , which is a factor of about 5 smaller than the value at which instabilities occur. A total of 34 h of Cray 2 computer time per run were needed.

Space permits giving here only the most salient results. Additional information will be given in Ref. [11]. Here we will focus on the analysis of our results for the quasi-static order-parameter correlation function  $C(\mathbf{r}, t)$ :

$$C(\mathbf{r}, t) = \langle \phi(\mathbf{r}, t) \phi(0, 0) \rangle, \quad (3)$$

which can be used to characterize the order-parameter growth. Additionally, we have obtained the current correlation functions  $C_{ik}(\mathbf{r}) \equiv \langle j_i(\mathbf{r}, t) j_k(0, 0) \rangle$ . As in the two-dimensional case,  $C_{ik}$  reaches, in a relatively short time, its equilibrium value as given by the equipartition theorem. It contains no information on order growth, which is contained in  $C(\mathbf{r}, t)$  [or its Fourier transform  $C(\mathbf{K}, t)$ ]. We consider here specifically  $C(r, t)$ , the spherically averaged value of  $C(\mathbf{r}, t)$ .

Our results for  $C(r, t)$  are shown in Fig. 1 at suitable time intervals. We note the growth of local order ( $r=0$  peak height) as well as the order range. We will characterize the latter by  $l(t) = R(t)$ , where  $R(t)$  is defined as the first zero of  $C(r, t)$ . We will show below that  $C(r, t)$  scales in the later part of the time range considered. Other measures of order range will be dealt with in Ref. [11].

In Fig. 2 we show our results for  $R(t)$  vs  $t$  over the entire range studied. In this figure [which can be contrasted with the corresponding Fig. 8 of Ref. [7] or Fig. 14 of Ref. [6] for the purposes of comparing with the same model in two-dimensions or with the three-dimensional model B] we see that  $R(t)$  has an initial region of relatively slow growth, followed by a faster region. This is the same as in two-dimensions. However, it is not possible now to derive a value of  $n$  at the longer times studied by fitting a straight line through the last points in the time range. Defining a time-dependent exponent  $n(t)$  by the expression  $n(t) = d \ln R(t) / d \ln t$  for example, one finds that  $n(t)$  increases throughout the time range studied, without any signs of saturation. This is in contrast to the two-dimensional case, where, towards the end of the runs, any change in the effective exponent was not obvious.

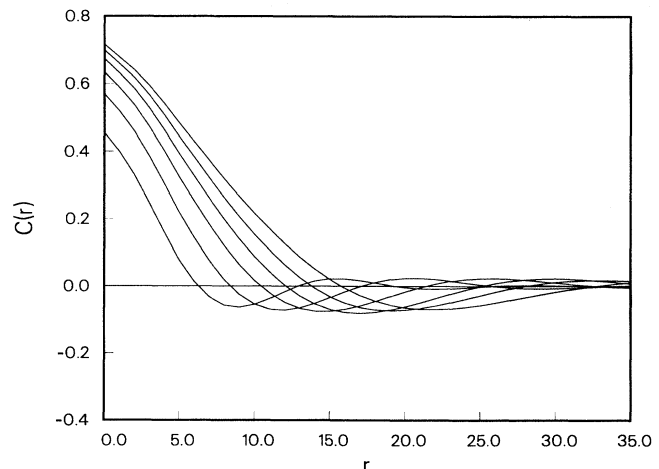


FIG. 1. The spherically averaged order-parameter correlation function  $C(r)$ , as a function of  $r$ , at times 50, 100, 150, 200, 250, and 300.

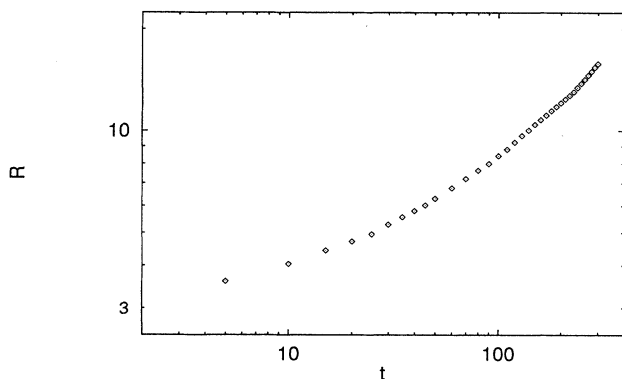


FIG. 2. The first zero of  $C(r,t)$  as a function of time. Note that the growth exponent is increasing with time.

Thus, to study the behavior of the system at long times we turn to the procedure employed in Ref. [12] of plotting an effective exponent  $n(t)$  versus the corresponding value of  $1/R(t)$  and looking for the trend as the value of  $1/R(t)$  decreases towards zero. This is done in Fig. 3. The exponent value plotted there is obtained from a best straight-line fit to the three points in Fig. 2 centered around the value of  $R(t)$  considered. The rather large error bars in the plot arise, obviously, from the relatively small number of runs considered here. However, the trend is rather clear: at a value of  $R$  which corresponds to a time  $t \approx 80-100$  (in our dimensionless measure) a marked increase in  $n$  becomes evident. At earlier times  $n$  is much flatter [13]. We have fitted a straight line, therefore, through all data points in the range  $90 \leq t < 300$ , and this line is indicated in Fig. 3. The intercept with the  $y$  axis, which we identify with the asymptotic value of  $n$ , is 0.99 in excellent agreement with the value of unity expected from phenomenological considerations [14]. This is in contrast with the two-dimensional results [7] where  $n$  appears to saturate.

Finally, we briefly consider scaling. We replot the correlation function  $C(r,t)$  as a function of  $x = r/R(t)$ . In the scaling regime the scaling function  $f(x)$  defined as

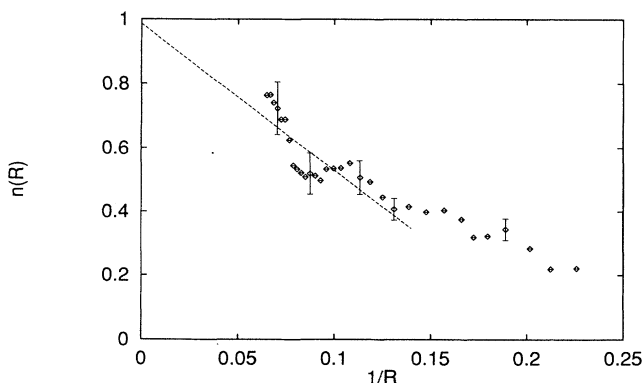


FIG. 3. The effective growth exponent  $n(R(t))$ , as defined in the text, plotted against  $1/R(t)$ . The straight line is a best fit to all times  $t \geq 90$ , and it intercepts the  $y$  axis at  $n = 0.99$ .

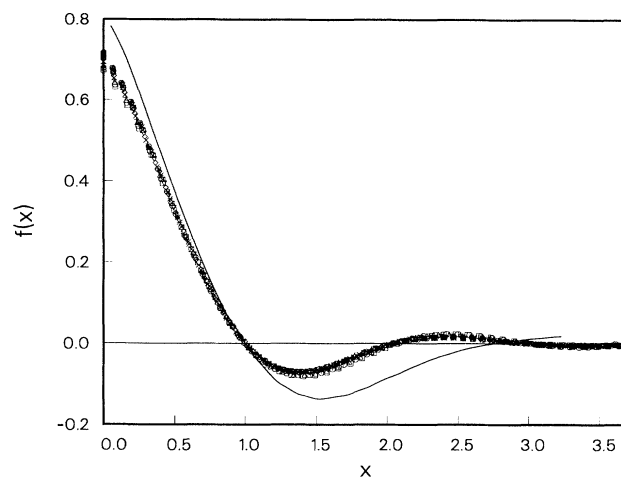


FIG. 4. The scaling function  $f(x)$  as defined in Eq. (4) plotted for 11 times between  $t=200$  and  $t=300$ . The solid line shows, for comparison, the  $d=2$  scaling function (Ref. [7]).

$$C(r,t) = f(r/R(t)) = f(x) \tag{4}$$

should be independent of  $t$ . The function  $f$  is plotted in Fig. 4 for 11 values of  $t$  ranging from  $t=200$  to  $t=300$ . Although this is a rather limited range, we see that the data appear to scale quite well, despite the fact that  $n$  is clearly still changing in the time range plotted. Indeed scaling is better, particularly at small  $x$ , than in the corresponding range at  $d=2$  (Ref. [7]). We note that such scaling behavior is attained, in the case of model B quenches to zero temperature [5], only at fairly long times (roughly  $t \sim 500$  in our units) [15]. Assuming that the function plotted can indeed be identified with the scaling function, it is instructive to examine its dimensionality dependence. By comparing with Ref. [7] we see that the dimensionality effect is quite considerable: the three-dimensional function has a shallower first minimum, a lower secondary maximum and a considerably smaller value of the second zero than that found in the two dimensions. The reasons for this are not clear but we can point out that the scaling function for model B exhibits similar trends when going from two [16] to three [6] dimensions.

It is worthwhile to emphasize here the most salient differences between this work and that of Ref. [9], where linear growth in time is also reported. In the paper by Koga and Kawasaki, a very different model is studied where the currents are modeled by an interaction involving the order parameter which is nonlocal in space. The physical interpretation and relation to phenomenology of that model are difficult. The system size used there is only  $N=64$ . The model used by Pori and Dunweg is a simplified version of the one used here, with the temperature set to zero and the nonlinear convective terms, in (1b) dropped for the sake of computational simplification. There is no argument that shows that these terms are irrelevant to spinodal decomposition. They use  $N=80$  but the maximum size of  $l(t)$  they attain is smaller than ours. Thus, we believe our study is more complete and physically realistic.

In summary, we have obtained results for spinodal decomposition after a critical quench to nonzero temperature for a three-dimensional fluid model which includes the full couplings between order parameter and currents. Our results agree with the phenomenological expectation

that the asymptotic growth exponent is unity. This is our main result. When compared with the two-dimensional results for exactly the same model, they support the contention that the dimensionality [17] may be relevant to the fluid problem.

- 
- [1] See, for example, N. Wong and C. Knobler, *Phys. Rev. A* **24**, 3205 (1981); E. Siebert and C. Knobler, *Phys. Rev. Lett.* **54**, 819 (1985); Y. C. Chou and W. I. Goldberg, *Phys. Rev. A* **20**, 2015 (1979); F. S. Bates and P. Wiltzius, *J. Chem. Phys.* **91**, 3258 (1989).
- [2] See among others S. Komura *et al.*, *Phys. Rev. B* **31**, 1278 (1985); S. Katami and M. Iizumi, *Phys. Rev. Lett.* **52**, 835 (1984); M. Hennion *et al.*, *Acta Metall.* **30**, 599 (1982).
- [3] E. Siggia, *Phys. Rev. A* **20**, 595 (1979).
- [4] P. C. Hohenberg and B. I. Halperin, *Rev. Mod. Phys.* **49**, 135 (1977).
- [5] T. M. Rogers, K. R. Elder, and R. C. Desai, *Phys. Rev. B* **37**, 9638 (1988); O. T. Valls and G. F. Mazenko, *ibid.* **38**, 11650 (1988); E. T. Gawlinski *et al.*, *ibid.* **39**, 7266 (1989).
- [6] A. Chakrabarti *et al.*, *Phys. Rev. B* **39**, 4386 (1985).
- [7] J. E. Farrell and O. T. Valls, *Phys. Rev. B* **40**, 7027 (1989); **43**, 630 (1991).
- [8] J. E. Farrell and O. T. Valls, *Phys. Rev. B* **42**, 2353 (1990).
- [9] T. Koga and K. Kawasaki, *Phys. Rev. A* **44**, R817 (1991) and S. Puri and B. Dunweg, *ibid.* **45**, R6977 (1992), have reported results for  $d=3$  fluids. The main differences between their work and ours are discussed below.
- [10] K. Kawasaki, *Ann. Phys. (N.Y.)* **61**, 1 (1970); M. J. Nolan, *Phys. Rev. B* **18**, 6334 (1978).
- [11] J. E. Farrell and O. T. Valls (unpublished).
- [12] D. A. Huse, *Phys. Rev. B* **34**, 7845 (1986).
- [13] The early time value of  $n$  is somewhat difficult to establish in this case. The region where  $n=0.3$  is not as extended as in  $d=2$ . The size of this region could be increased by decreasing the order parameter to current coupling,  $g$ , but this would make the study of the asymptotic region even harder.
- [14] The intercept value is not very sensitive to the starting point of the fit. Even starting the fit as early as  $t=60$  lowers the intercept only to 0.94.
- [15] The units employed in Ref. [6] are quite unrelated to those used here in Ref. [7]. The domain size at the end of our runs is actually larger than that attained for model B.
- [16] M. San Miguel *et al.*, *Phys. Rev. A* **31**, 1001 (1985).
- [17] Some caution is needed here: we are comparing our three-dimensional extrapolated  $n$  with a finite-time two-dimensional value. As explained in the last section of Ref. [7], that value cannot be conclusively taken to be the confirmed asymptotic value.